

Tellurium *n*-type doping of highly mismatched amorphous GaN_{1-x}As_x alloys in plasma-assisted molecular beam epitaxy.

S. V. Novikov¹, M. Ting^{2,3}, K. M. Yu², W. L. Sarney⁴, R. W. Martin⁵, S. P. Svensson⁴, W. Walukiewicz² and C. T. Foxon¹

¹*School of Physics and Astronomy, University of Nottingham, Nottingham NG7 2RD, UK*

²*Materials Sciences Division, Lawrence Berkeley National Laboratory, Berkeley, CA 94720, USA*

³*Department of Mechanical Engineering, University of California, Berkeley, CA 94720*

⁴*US Army Research Laboratory, Adelphi, MD 20783, USA*

⁵*Department of Physics, SUPA, University of Strathclyde, Glasgow, G4 0NG, UK*

- We report on *n*-type doping of amorphous GaN_{1-x}As_x layers with Te in PA-MBE.
- We have used a low temperature PbTe source as a source of tellurium.
- Reproducible Te incorporation in amorphous GaN_{1-x}As_x layers has been achieved.
- The optimal growth temperature window for efficient Te doping has been determined.

Tellurium n -type doping of highly mismatched amorphous $\text{GaN}_{1-x}\text{As}_x$ alloys in plasma-assisted molecular beam epitaxy.

S. V. Novikov¹, M. Ting^{2,3}, K. M. Yu², W. L. Sarney⁴, R. W. Martin⁵, S. P. Svensson⁴, W. Walukiewicz² and C. T. Foxon¹

¹*School of Physics and Astronomy, University of Nottingham, Nottingham NG7 2RD, UK*

²*Materials Sciences Division, Lawrence Berkeley National Laboratory, Berkeley, CA 94720, USA*

³*Department of Mechanical Engineering, University of California, Berkeley, CA 94720*

⁴*US Army Research Laboratory, Adelphi, MD 20783, USA*

⁵*Department of Physics, SUPA, University of Strathclyde, Glasgow, G4 0NG, UK*

*e-mail: Sergei.Novikov@Nottingham.ac.uk

Abstract.

In this paper we report our study on n -type Te doping of amorphous $\text{GaN}_{1-x}\text{As}_x$ layers grown by plasma-assisted molecular beam epitaxy. We have used a low temperature PbTe source as a source of tellurium. Reproducible and uniform tellurium incorporation in amorphous $\text{GaN}_{1-x}\text{As}_x$ layers has been successfully achieved with a maximum Te concentration of $9 \times 10^{20} \text{ cm}^{-3}$. Tellurium incorporation resulted in n -doping of $\text{GaN}_{1-x}\text{As}_x$ layers with Hall carrier concentrations up to $3 \times 10^{19} \text{ cm}^{-3}$ and mobilities of $\sim 1 \text{ cm}^2/\text{Vs}$. The optimal growth temperature window for efficient Te doping of the amorphous $\text{GaN}_{1-x}\text{As}_x$ layers has been determined.

Keywords:

A3. Molecular beam epitaxy

B1. Nitrides

B2. Semiconducting III-V materials

PACS: 81.15.Hi, 81.05.Ea.

Introduction

In the so-called highly mismatched alloys (HMAs) the band anticrossing (BAC) model predicts that a wide range of direct energy gaps can be achieved through the modification of the conduction and valence bands [1,2]. For example, the energy gap of highly mismatched $\text{GaN}_{1-x}\text{As}_x$ alloys is expected to vary from 0.7 eV to 3.4 eV. An even larger modification of the electronic band structure is expected for the more extremely mismatched $\text{GaN}_{1-x}\text{Sb}_x$ and $\text{GaN}_{1-x}\text{Bi}_x$ alloys [1-3]. The large band gap range and controllable conduction and valence band edge positions make HMAs promising materials for solar energy conversion devices. For example, the HMAs may be suitable photoelectrodes for photoelectrochemical solar water splitting. This application requires a semiconductor with the bandgap of about >2.0 eV and the conduction and valence band edges straddling the H_2O redox potentials. At dilute doping levels, As, Sb and Bi form localized energy levels above the valence band in GaN. Our measurements of GaN doped with As and Sb have demonstrated that the localized As and the Sb levels lie at about 0.7 eV and 1.2 eV above the valence band edge of GaN, respectively [4,5]. The BAC model predicts that at higher concentrations of these group V elements the

interaction of the localized states with the valence band of GaN results in formation of a fully occupied narrow band of extended states that plays the role of a new valence band edge [1,2]. This has been shown to result in an abrupt reduction of the optical gap of the HMAs.

Previously we have achieved an enhanced incorporation of As, Sb and Bi in GaN by growing the alloy thin films at extremely low temperatures (down to about 100 °C) by plasma-assisted (PA-MBE) [6-11]. Although the layers become amorphous for high As, Sb and Bi content, optical absorption measurements are consistent with the predictions of the BAC model, indicating that the amorphous HMAs samples have a short-range order resembling random crystalline alloys. The large band gap range and controllable positions of the conduction and valence bands make these HMAs promising materials for efficient solar energy conversion devices. However, before such devices can be realised, it is essential to achieve controlled *n*- and *p*-doping of GaN_{1-x}As_x alloys over a large composition range.

Recently, we have demonstrated a successful *p*-type doping of amorphous GaN_{1-x}As_x alloys with Mg [12]. The room temperature *p*-type conductivity has increased monotonically with increasing of Mg content, up to a maximum value of about 4.86 S/cm for 8 atomic % Mg content. We have found that achieving the *p*-type conductivity of GaN_{1-x}As_x layers, requires growth under Ga-rich conditions [12]. These conditions result in the formation of As-rich crystalline GaAs:N inclusions inside the amorphous GaN_{1-x}As_x matrix, which can be observed in the X-ray diffraction (XRD) and transmission electron microscopy (TEM) [12]. The role of these inclusions on the hole transport will require further studies. However, since the fraction of the GaAs:N is relatively low we believe the hole transport predominantly occurs in the As derived valence band of GaN_{1-x}As_x.

We have also shown that it is possible to achieve *n*-type doping of amorphous GaN_{1-x}As_x alloys with Te [12]. In MBE studies of GaAs:Te it was demonstrated many years ago that tellurium tends to accumulate on the surface by displacing arsenic atoms and forming a stable surface compound, presumably GaTe [13,14]. The build-up of a high surface concentration of Te on GaAs during MBE growth makes the doping process extremely difficult to control. However, Te doping in GaAs has been successfully achieved using PbTe as a doping source [13,14]. This is because Pb itself has a unity sticking coefficient on GaAs at room temperatures, but rapidly desorbs at temperatures above 250 °C.

In this paper we present a systematic study of the growth conditions affecting Te doping of amorphous GaN_{1-x}As_x layers grown by PA-MBE. We show that controlling of the fluxes of Te and As and the growth temperatures are essential for efficient *n*-doping of the GaN_{1-x}As_x alloy with specific composition.

II. EXPERIMENTAL DETAILS

GaN_{1-x}As_x samples were grown by plasma-assisted molecular beam epitaxy (PA-MBE) in a MOD-GENII system. The system has a HD-25 Oxford Applied Research RF activated plasma source to provide active nitrogen and elemental Ga is used as the group III-source. In all experiments we have used arsenic in the form of As₂ produced by a Veeco arsenic valved cracker. A low temperature PbTe source has been installed in the system for the studies of *n*-type doping. The MBE system is equipped with reflection high energy electron diffraction (RHEED) for surface reconstruction analysis. For the growth of all GaN_{1-x}As_x samples, we have used the same active nitrogen flux (total N₂ beam equivalent pressure (BEP) $\sim 1.5 \times 10^{-5}$ Torr, RF power 200 W) and the same deposition time of 2 hours. All layers were grown on 2-inch (0001)

sapphire substrates.

Note that in MBE the substrate temperature is normally measured using an optical pyrometer. However, because we have used uncoated transparent sapphire the pyrometer measures the temperature of the substrate heater, but not the substrate. Therefore in this study our estimate of the growth temperature is based on a thermocouple reading [6-9].

We have used a wide range of *in-situ* and *ex-situ* characterisation techniques to study the surface morphology, composition, structural, electrical and optical properties of the GaN_{1-x}As_x:Te layers. The morphology of the samples was studied *in-situ* using RHEED and *ex-situ* using atomic force microscopy (AFM). The structure and orientation of the GaN_{1-x}As_x layers were determined by X-ray diffraction (XRD) using a Philips X'Pert MRD diffractometer. Microstructural information on the GaN_{1-x}As_x alloys was obtained using transmission electron microscopy (TEM) techniques. Microscopic crystallinity and phase separation were studied by directly comparing the selective area electron diffraction patterns (SAD) with XRD measurements. The As content and uniformity in the GaN_{1-x}As_x films were measured by electron probe microanalysis (EPMA) using a Cameca SX100 and by combined Rutherford backscattering spectrometry (RBS) and particle-induced x-ray emission (PIXE) measurements using a 3.04 MeV ⁴He⁺⁺ beam. The band gap of the thin films was measured by optical transmission and reflection using a Perkin Elmer Lambda 950 Spectrophotometer over the wavelength range of 190-3000 nm. Hall effect measurements in the van der Pauw configuration were used to determine the electrical properties of the deposited films.

III. RESULTS AND DISCUSSION

In order to achieve *n*-type conductivity in Te-doped amorphous GaN_{1-x}As_x, the layers have to be grown under Ga-rich conditions as described above. Therefore, in the current study we used a constant Ga flux with a BEP $\sim 2 \times 10^{-7}$ Torr and operated the HD-25 nitrogen source at 200W with a N₂ BEP of $\sim 1.5 \times 10^{-5}$ Torr. The arsenic flux range was selected in order to maintain the composition of the GaN_{1-x}As_x layers at around 60 mol%. Initially we grew several sets of samples at a growth temperature of ~ 280 °C with an As BEP of $\sim 6 \times 10^{-6}$ Torr. RBS data confirms that the GaAs content in this set of layers was about 60 mol% ($x \sim 0.6$) and the optical band gap of the GaN_{1-x}As_x layers was ~ 1.3 eV as measured by absorption studies. The RHEED patterns demonstrated the formation of an amorphous layer during the first few minutes of the growth. The GaN_{1-x}As_x layers remained amorphous during the whole duration of the growth. Different fluxes of PbTe were used in order to investigate *n*-type doping, but we did not observe any significant changes in the RHEED pattern for the entire range of PbTe fluxes studied.

RBS data demonstrate a uniform incorporation of tellurium through the bulk of the GaN_{1-x}As_x:Te layers. Figure 1 shows the dependence of the Te concentration in the GaN_{1-x}As_x layers measured by RBS against the PbTe flux. The thickness of the GaN_{1-x}As_x:Te layers was in the range 0.6 - 1 μm as measured by RBS, with the majority of the layers having a thickness ~ 0.9 μm . We have observed a gradual increase of the Te incorporation up to $\sim 4 \times 10^{20}$ cm⁻³ as the PbTe flux increased. At the same time the RBS measurements show that Pb is not efficiently incorporated into the bulk of the GaN_{1-x}As_x layers, with Pb concentration lower than 1.3×10^{20} cm⁻³ for the highest PbTe fluxes.

XRD measurements on these samples did not show any GaN related peaks, confirming the amorphous structure of the grown GaN_{1-x}As_x layers. However, as we have reported previously

[12], a weak feature corresponding to the (111) diffraction peak of zinc blende GaAs:N can be detected. This indicates the presence of small crystalline GaAs:N inclusions in the amorphous GaN_{1-x}As_x:Te film. The presence of these inclusions has been confirmed by detailed TEM results that will be published separately.

Figure 2 presents dependence of the resistivity and electron concentration as a function of the Te concentration measured by RBS. Hall effect measurements demonstrate that both undoped and Te-doped GaN_{1-x}As_x layers exhibit *n*-type conductivity. The resistivity drops abruptly for Te concentrations above 10¹⁹ cm⁻³. At the same time we observe an increase in the electron concentrations up to 6×10¹⁸ cm⁻³. For Te doping higher than 2×10²⁰ cm⁻³, a decrease in the electron concentration is observed. This may suggest deactivation of Te donors or formation of compensating native defects at this high Te doping level. The electron mobilities for all of the Te doped samples are very low, ranging from 0.4 - 1.1 cm²/Vs. These values are reasonable given the amorphous structure of the GaN_{1-x}As_x matrix.

Since the electrically active Te donors substitute the anion sites it is expected that the efficiency of the Te incorporation will depend on the As to N ratio. We have studied the influence of the As₂ flux during growth on the efficiency of the Te doping by changing the As₂ flux BEP from 1.0×10⁻⁶ Torr to 6.4×10⁻⁶ Torr. The lower range of arsenic fluxes was limited to 1.0×10⁻⁶ Torr to avoid the formation of metallic droplets on the surface of the GaN_{1-x}As_x:Te layers. Figure 3a shows tellurium incorporation measured by RBS as a function of the Te flux used during the growth for three different arsenic fluxes. For all three As₂ fluxes we have achieved efficient incorporation of Te into the GaN_{1-x}As_x layers. We observed a gradual increase of the Te incorporation as the PbTe flux increased. At the same time there is a clear increase in Te incorporation with decreasing As₂ flux. The maximum Te concentration achieved at the

lowest arsenic flux was $\sim 9 \times 10^{20} \text{ cm}^{-3}$.

Further evidence for a complex interrelatedness between different growth parameters is shown in Figure 3b that presents RBS measured GaAs mole percent in $\text{GaN}_{1-x}\text{As}_x\text{:Te}$ layers as a function of PbTe flux for 3 different arsenic fluxes. At high arsenic fluxes the Te incorporation does not have a significant influence on the alloy composition of the $\text{GaN}_{1-x}\text{As}_x$ layers. The constant composition of about 60% GaAs mole fraction is close to the intended composition set by the As and N fluxes. It is worth noting that at this composition $\text{GaN}_{1-x}\text{As}_x$ has the direct energy gap of 1.5 eV, which is close the optimum gap for efficient utilization of the solar spectrum. At the lowest As_2 flux of $\text{BEP} \sim 1.0 \times 10^{-6}$ Torr we have observed a clear decrease in the arsenic incorporation with increasing PbTe fluxes. This behaviour could be understood by noting that the Ga-N bond (2.24 eV/bond [15]) is significantly stronger than the Ga-As bond (1.63 eV/bond [15]). As a result there is a preferential incorporation of nitrogen over arsenic in the $\text{GaN}_{1-x}\text{As}_x$ layers. We were unable to find reliable published data on the energy of the Ga-Te bond. We expect that the value must be higher than that for the Ga-As bond, because the experimental data demonstrate that Te replaces As on the growth surface during MBE of GaAs:Te [13,14]. Therefore, we suggest that at low arsenic fluxes the probability of bonding Te to Ga increases due to the higher quantity of free Ga atoms on the growth surface. This will result in an increase of tellurium incorporation and in a decrease in the arsenic incorporation to $\text{GaN}_{1-x}\text{As}_x\text{:Te}$ layers. Therefore, the need to control the alloy composition requires high enough As_2 fluxes. Consequently, although the low As_2 flux of 1.2×10^{-6} Torr improves the Te incorporation it does not allow a control of the $\text{GaN}_{1-x}\text{As}_x$ alloy composition.

Resistivities of the $\text{GaN}_{1-x}\text{As}_x\text{:Te}$ films as a function of PbTe BEP grown under different As fluxes are shown in Figure 4. The figure demonstrates that we can reproducibly control *n*-type

doping of GaN_{1-x}As_x layers by changing the PbTe flux during growth for the whole range of arsenic fluxes studied. Increasing PbTe flux during the MBE growth increases Te incorporation and resulting in a decrease of the resistivity. The observed behaviour is similar for the 3 different arsenic fluxes. The lowest resistivity is observed for the lowest arsenic flux and that probably relates to the highest Te incorporation under these growth conditions as shown in Fig.3a. We have demonstrated Hall electron concentrations in the GaN_{1-x}As_x layers up to $3 \times 10^{19} \text{cm}^{-3}$. It should be noted however that the reduced resistivity of the film grown at the lowest As₂ flux comes at the price of reduced capability to control the alloy composition that is essential for all practical applications of GaN_{1-x}As_x. The electron mobility in all samples was weakly dependent on the doping level and remained very low at $\sim 1 \text{ cm}^2/\text{Vs}$.

Finally we have investigated the effect of the PA-MBE growth temperature on the electrical properties of the Te doped GaN_{1-x}As_x. For this study we have used constant As₂ flux of $3.2 \times 10^{-6} \text{ Torr}$ that, as is shown in Figs. 3 and 4 has provided alloy with well defined composition and good electrical properties. Figure 5 presents dependencies of the Te concentration and alloy composition on the temperature for fixed As₂ and Te fluxes. There is a fixed temperature growth window where we can achieve *n*-type doping of GaN_{1-x}As_x with PbTe flux. At growth temperatures below $\sim 250 \text{ }^\circ\text{C}$ we cannot see any effect of the PbTe flux on the transport properties of GaN_{1-x}As_x layers, probably because the temperature of the surface is too low for decomposition of the PbTe. This temperature is practically identical to the minimum growth temperatures for efficient Te doping of GaAs layers in MBE [13,14]. Also, as shown in Fig. 5, we have observed a decrease in the incorporation of Te and As in GaN_{1-x}As_x at growth temperatures above $\sim 400 \text{ }^\circ\text{C}$. This is consistent with our previous papers on the growth of amorphous GaN_{1-x}As_x layers that have shown reduced incorporation of As with increasing growth temperature [6,7]. However, it is still unclear whether the decrease in

the Te incorporation with increasing growth temperature is related to the reduced arsenic incorporation at higher growth temperatures.

Results in Fig 6 show the temperature dependence of the resistivity for the samples from Fig. 5. The low resistivity is obtained only for the growth temperatures between 280 °C and 330 °C. At temperature higher than 350 °C the resistivity increases abruptly by more than an order of magnitude indicating increasing fraction of electrically inactive Te atoms in the material.

Conclusions

In this paper we have studied *n*-type Te doping of amorphous GaN_{1-x}As_x layers grown by PA-MBE. A low temperature PbTe was used as a source of tellurium. We have carried out a systematic investigation of the effects of varying Te and As fluxes as well as the substrate temperature on a growth of GaN_{1-x}As_x films with controlled *n*-type conductivity. We have successfully identified the range of the growth parameters for reproducible and uniform tellurium incorporation in amorphous GaN_{1-x}As_x layers with $x \sim 0.6$. Tellurium incorporation resulted in *n*-doping of GaNAs layers with resistivity changes over 4 orders of magnitude, Hall electron concentrations up to $3 \times 10^{19} \text{ cm}^{-3}$ and mobilities of $\sim 1 \text{ cm}^2/\text{Vs}$. The optimal temperature growth window for efficient Te incorporation into GaN_{1-x}As_x layers was found to be between 250 °C and 400 °C, although the highest *n*-type conductivity has been observed in a more limited temperature range from 280 °C to ~ 330 °C. The successful synthesis of *n*-type doped GaN_{1-x}As_x provides a unique opportunity to study doping and charge transport in ionic amorphous material. Also in combination with previously reported *p*-type doping it offers a potential for realizing *p-n* junction in a non-crystalline semiconductors.

Acknowledgements

This work was undertaken with support from the EPSRC UK, under grant numbers EP/I004203/1 and EP/I00467X/1. The MBE growth at Nottingham was also supported by the US Army Foreign Technology Assessment Support (FTAS) program. The characterization work performed at LBNL was supported by the Director, Office of Science, Office of Basic Energy Sciences, Materials Sciences and Engineering Division, of the U.S. Department of Energy under Contract No. DE-AC02-05CH11231.

References

- [1] J. Wu, W. Walukiewicz, K. M. Yu, J. D. Denlinger, W. Shan, J. W. Ager, A. Kimura, H. F. Tang, T. F. Kuech, *Phys Rev B* 70 (2004) 115214.
- [2] W. Walukiewicz, K. Alberi, J. Wu, W. Shan, K. M. Yu, J. W. Ager III, in *Physics of Dilute III-V Nitride Semiconductors and Material Systems: Physics and Technology*, edited by Ayse Erol (Springer-Verlag Berlin-Heidelberg 2008) Chapter 3.
- [3] R. M. Sheetz, E. Richter, A. N. Andriotis, S. Lisenkov, C. Pendyala, M. K. Sunkara, M. Menon, *Phys. Rev. B* 84 (2011) 075304.
- [4] C. T. Foxon, I. Harrison, S. V. Novikov, A. J. Winser, R. P. Campion, T. Li, *J. of Physics: Condensed Matter* 14 (2002) 3383.
- [5] S. V. Novikov, K. M. Yu, W. L. Sarney, Z. Liliental-Weber, M. Ting, R. E. L. Powell, M. Shaw, A. J. Kent, R. W. Martin, S. P. Svensson, W. Walukiewicz, C. T. Foxon, in *Proc.: 2013 Materials Research Society Fall Meeting, Boston, USA, December 1-6, 2013*, P.253.
- [6] S. V. Novikov, C. R. Staddon, A. V. Akimov, R. P. Campion, N. Zainal, A. J. Kent, C. T. Foxon, C. H. Chen, K. M. Yu, W. Walukiewicz, *J. Cryst. Growth* 311 (2009) 3417.
- [7] K. M. Yu, S. V. Novikov, R. Broesler, I. N. Demchenko, J. D. Denlinger, Z. Liliental-Weber, F. Luckert, R. W. Martin, W. Walukiewicz, C. T. Foxon, *J. Appl. Phys.*, 106 (2009) 103709.
- [8] A. X. Levander, S. V. Novikov, Z. Liliental-Weber, R. dos Reis, J. D. Denlinger, J. Wu, O. D. Dubon, C. T. Foxon, K. M. Yu, W. Walukiewicz, *J. Mater. Res.* 26 (2011) 2887.
- [9] S. V. Novikov, K. M. Yu, A. Levander, D. Detert, W. L. Sarney, Z. Liliental-Weber, M. Shaw, R. W. Martin, S. P. Svensson, W. Walukiewicz, C. T. Foxon *J. Vac. Sci. Technol. B*, 31 (2013) 03C102-1.

- [10] K. M. Yu, W.L. Sarney, S. V. Novikov, D. Detert, R. Zhao, J. Denlinger, S.P. Svensson, O. D. Dubon, W. Walukiewicz, C. T. Foxon, *Appl. Phys. Lett.* 102 (2013) 102104.
- [11] W.L. Sarney, S.P. Svensson, S.V. Novikov, K.M. Yu, W. Walukiewicz, C.T. Foxon, *J. Cryst. Growth* 383 (2013) 95.
- [12] A. X. Levander, S. V. Novikov, Z. Liliental-Weber, R. dos Reis, O. D. Dubon, J. Wu, C. T. Foxon, K. M. Yu, W. Walukiewicz, *J. Appl. Phys.* 110 (2011) 093702
- [13] J. De-Sheng, Y. Makita, K. Ploog, H. J. Queisser, *J. Appl. Phys.* 53 (1982) 999.
- [14] S. M. Newstead, T. M. Kerr, C. E. C. Wood, *J. Appl. Phys.* 66 (1989) 4184.
- [15] A. Harrison, *Electronic Structure and the Properties of Solids* (W.H. Freeman and Company, San Francisco, 1980), p. 176.

Figure Captions

Figure 1. Tellurium concentration in $\text{GaN}_{1-x}\text{As}_x\text{:Te}$ layers measured by RBS as a function of the PbTe flux (BEP) used in the growth. MBE growth temperatures were ~ 280 °C, Ga BEP $\sim 2.3 \times 10^{-7}$ Torr and As_2 BEP $\sim 6.4 \times 10^{-6}$ Torr.

Figure 2. Resistivity (a) and electron concentration (b) in $\text{GaN}_{1-x}\text{As}_x\text{:Te}$ layers as a function of Te concentration measured by RBS. MBE growth temperatures were ~ 280 °C, Ga BEP $\sim 2.3 \times 10^{-7}$ Torr and As_2 BEP $\sim 6.4 \times 10^{-6}$ Torr.

Figure 3. Tellurium concentration (a) and GaAs content (b) in $\text{GaN}_{1-x}\text{As}_x\text{:Te}$ layers as a function of the PbTe flux (BEP) used in the growth for 3 different arsenic fluxes. MBE growth temperatures were ~ 280 °C and Ga BEP $\sim 2.3 \times 10^{-7}$ Torr.

Figure 4. Resistivity of $\text{GaN}_{1-x}\text{As}_x\text{:Te}$ layers as a function of the PbTe flux (BEP) used in the growth for 3 different arsenic fluxes. MBE growth temperatures were ~ 280 °C and Ga BEP $\sim 2.3 \times 10^{-7}$ Torr.

Figure 5. RBS Tellurium concentration (left) and GaAs content (right) in $\text{GaN}_{1-x}\text{As}_x\text{:Te}$ layers as a function of MBE growth temperatures. Ga BEP $\sim 2.3 \times 10^{-7}$ Torr, PbTe BEP $\sim 1.1 \times 10^{-8}$ Torr and As_2 BEP $\sim 3.2 \times 10^{-6}$ Torr.

Figure 6. Resistivity of $\text{GaN}_{1-x}\text{As}_x\text{:Te}$ layers as a function of MBE growth temperatures. Ga BEP $\sim 2.3 \times 10^{-7}$ Torr, PbTe BEP $\sim 1.1 \times 10^{-8}$ Torr and As_2 BEP $\sim 3.2 \times 10^{-6}$ Torr.

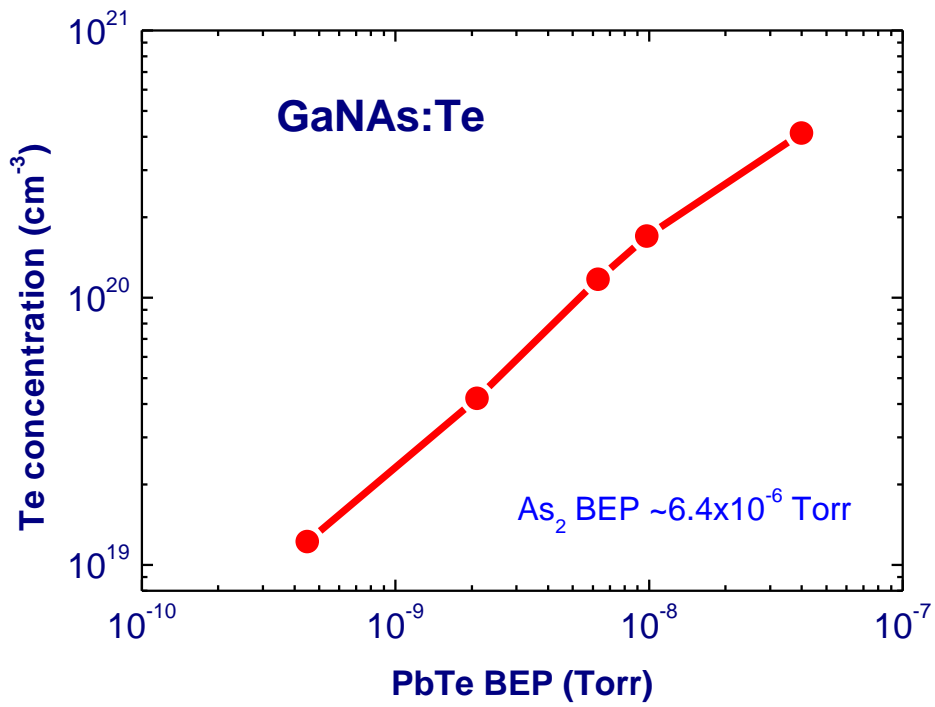


Figure 1. Tellurium concentration in GaN_{1-x}As_x:Te layers measured by RBS as a function of the PbTe flux (BEP) used in the growth. MBE growth temperatures were ~280 °C, Ga BEP ~2.3×10⁻⁷ Torr and As₂ BEP ~6.4×10⁻⁶ Torr.

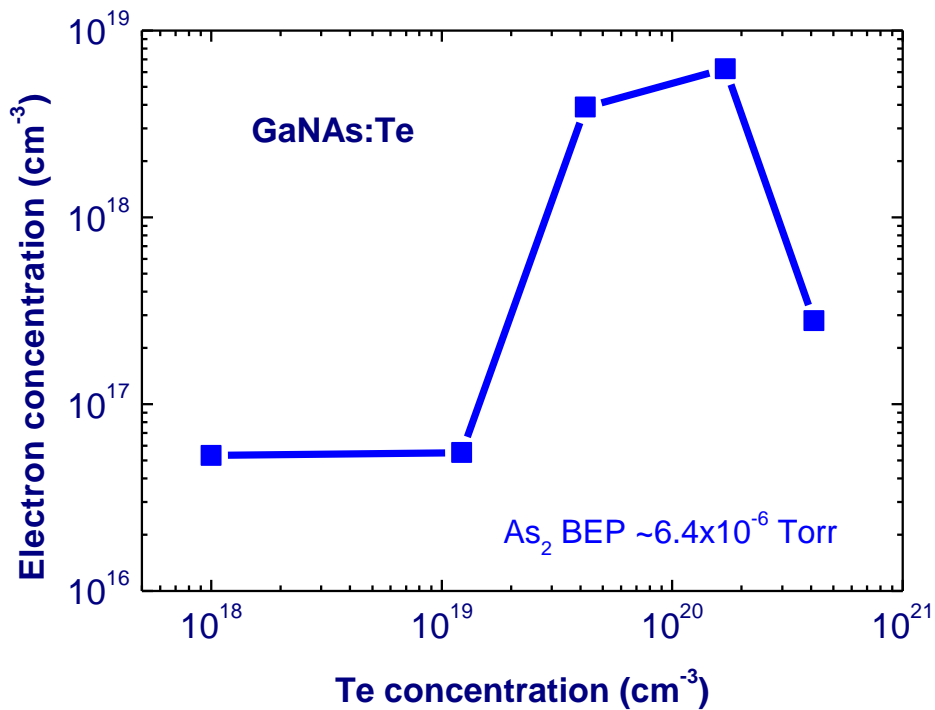
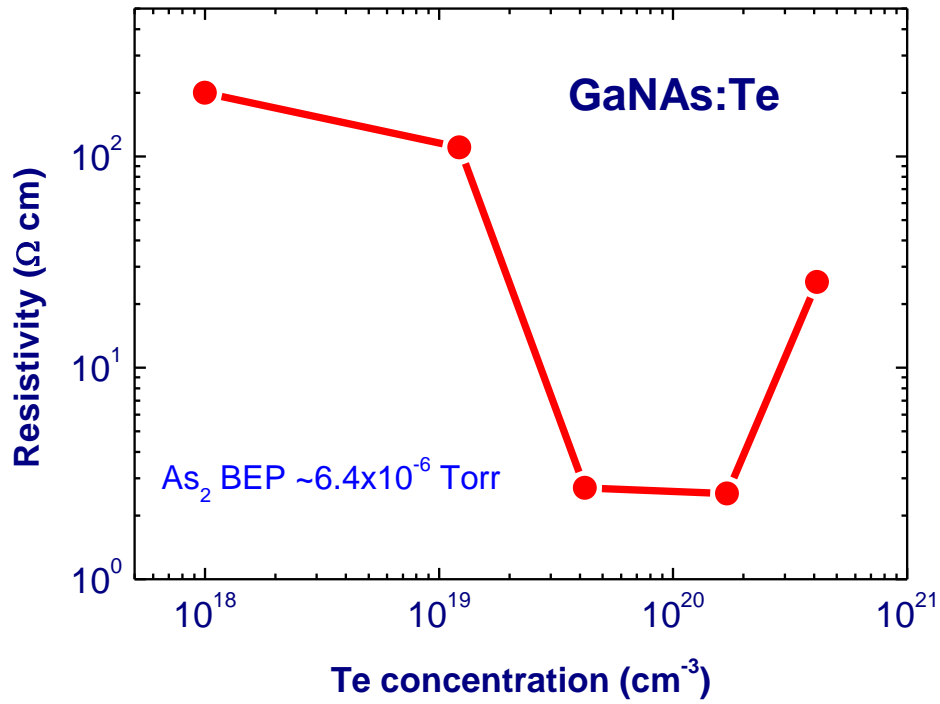


Figure 2. Resistivity (a) and electron concentration (b) in GaN_{1-x}As_x:Te layers as a function of Te concentration measured by RBS. MBE growth temperatures were ~280 °C, Ga BEP ~2.3×10⁻⁷ Torr and As₂ BEP ~6.4×10⁻⁶ Torr.

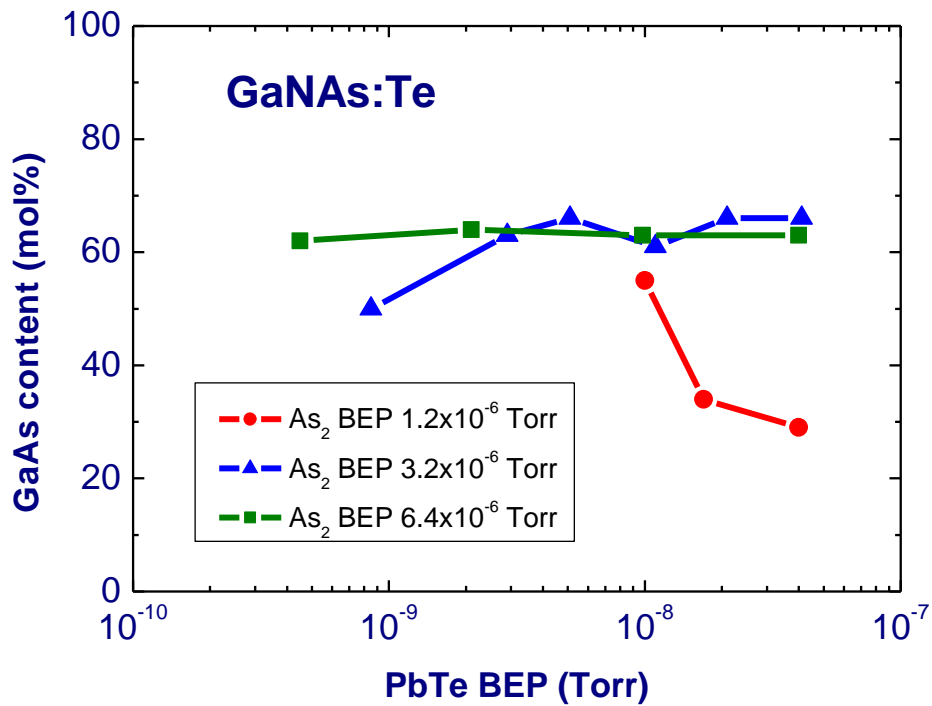
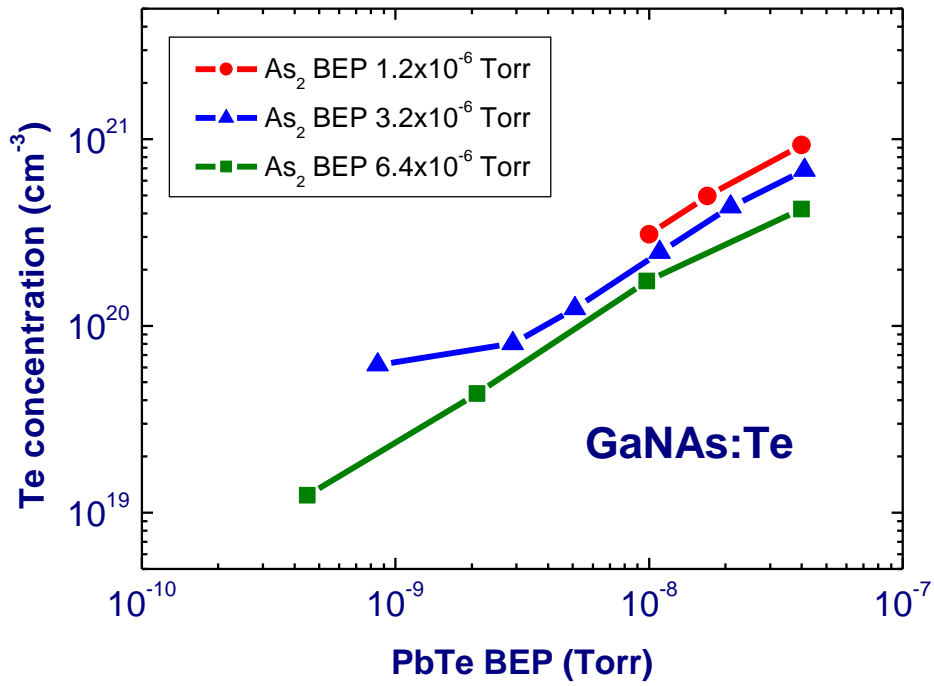


Figure 3. Tellurium concentration (a) and GaAs content (b) in $\text{GaN}_{1-x}\text{As}_x\text{:Te}$ layers as a function of the PbTe flux (BEP) used in the growth for 3 different arsenic fluxes. MBE growth temperatures were $\sim 280^\circ\text{C}$ and Ga BEP $\sim 2.3 \times 10^{-7}$ Torr.

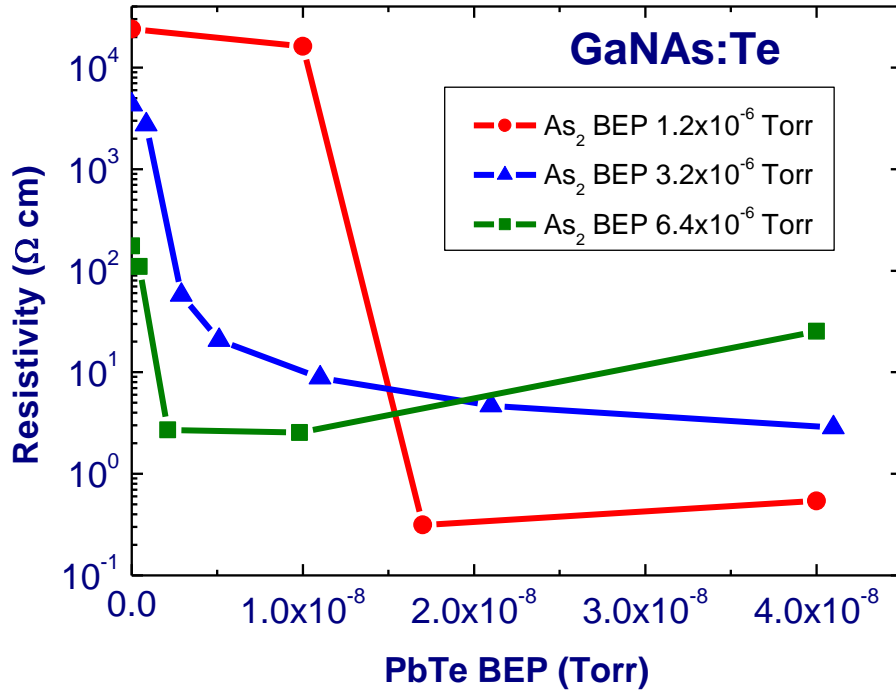


Figure 4. Resistivity of GaN_{1-x}As_x:Te layers as a function of the PbTe flux (BEP) used in the growth for 3 different arsenic fluxes. MBE growth temperatures were ~280 °C and Ga BEP ~2.3x10⁻⁷ Torr.

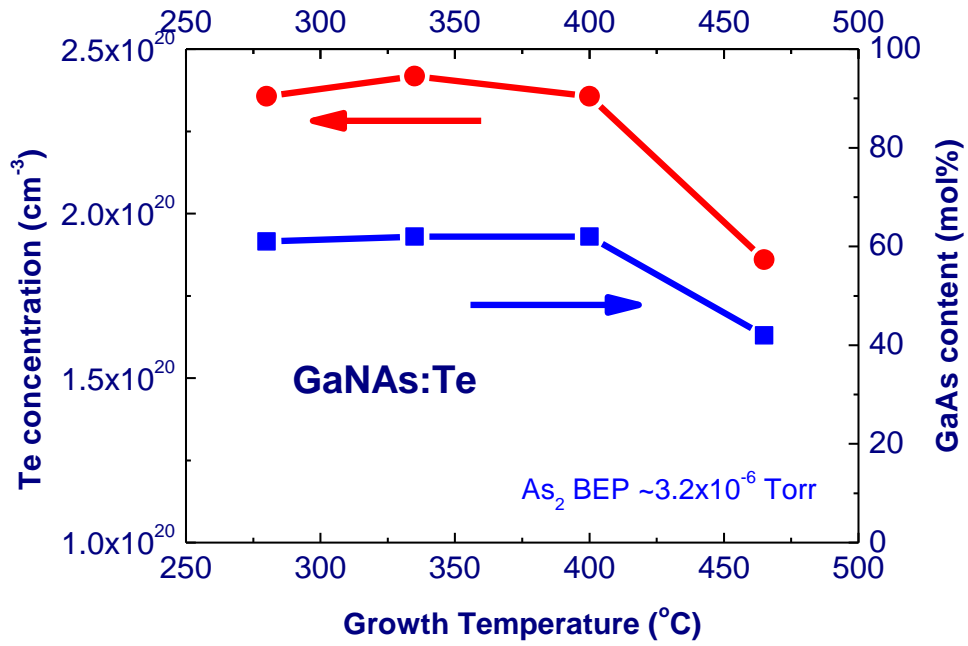


Figure 5. RBS Tellurium concentration (left) and GaAs content (right) in $\text{GaN}_{1-x}\text{As}_x\text{:Te}$ layers as a function of MBE growth temperatures. Ga BEP $\sim 2.3 \times 10^{-7}$ Torr, PbTe BEP $\sim 1.1 \times 10^{-8}$ Torr and As_2 BEP $\sim 3.2 \times 10^{-6}$ Torr.

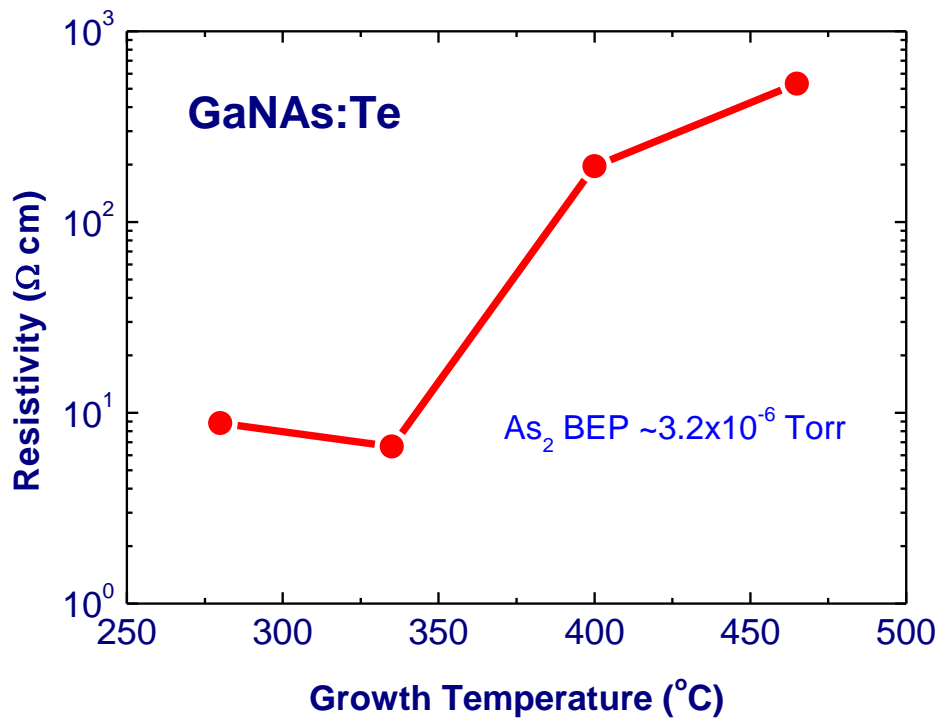


Figure 6. Resistivity of GaN_{1-x}As_x:Te layers as a function of MBE growth temperatures. Ga BEP $\sim 2.3 \times 10^{-7}$ Torr, PbTe BEP $\sim 1.1 \times 10^{-8}$ Torr and As₂ BEP $\sim 3.2 \times 10^{-6}$ Torr.